

J.H. SUNG<sup>✉</sup>  
J.Y. PARK  
T. IMRAN  
Y.S. LEE  
C.H. NAM

# Generation of 0.2-TW 5.5-fs optical pulses at 1 kHz using a differentially pumped hollow-fiber chirped-mirror compressor

Dept. of Physics and Coherent X-ray Research Center, Korea Advanced Institute of Science and Technology, Yusong, Daejeon 305-701, Korea

Received: 16 June 2005/Revised version: 1 August 2005  
Published online: 4 November 2005 • © Springer-Verlag 2005

**ABSTRACT** Optical pulses with 1.1-mJ energy and 5.5-fs duration have been generated at 1-kHz repetition rate from a chirped pulse amplification Ti:Sapphire laser incorporating a differentially pumped hollow-fiber chirped-mirror compressor. The effects of self-focusing and multi-photon ionization during the beam propagation were minimized by differentially pumping the hollow fiber filled with neon. The spectral broadening at the hollow-fiber compressor was optimized by adjusting gas pressure, laser intensity, and laser chirp, covering from 540 nm to 950 nm.

PACS 42.65.Jx; 42.65.Re

## 1 Introduction

Chirped pulse amplification (CPA) Ti:sapphire lasers have become a standard laser configuration for the generation of high-power femtosecond laser pulses. Lasers with duration as short as 20 fs and peak power of terawatt level are now feasible at 1-kHz repetition rate from CPA lasers [1]. High-power sub-10-fs optical pulses, however, cannot be generated directly from CPA lasers because the large gain required in them leads to serious gain narrowing. Thus generation of intense few-cycle laser pulses requires an additional technique after amplification. A hollow-fiber pulse compressor filled with noble gases has been recognized as a powerful technique in generating high-power sub-10-fs optical pulses [2–4]. When laser pulses generated in the CPA Ti:sapphire laser system are launched into a gas-filled hollow fiber, the self phase modulation (SPM) induced by optical Kerr effect in the gas causes spectral broadening and thus few-cycle pulses can be generated through chirp compensation of the continuum. In the hollow-fiber system with a constant gas pressure, the energy of few-cycle pulses is limited to sub-mJ because of the self-focusing and multi-photon ionization which produce spatial and spectral phase distortions and loss of the fundamental mode during the propagation through the hollow fiber [5, 6].

In order to further increase the energy of few-cycle pulses additional amplifier stages can be used after the hollow-fiber

compressor. A three-stage, 1-kHz amplifier system delivering pulses shorter than 10 fs with a peak power in excess of 0.3 TW was developed [7]. In this system the continuum energy was increased to 3.5 mJ by using two amplifier stages after the hollow-fiber system with a constant gas pressure. The use of the amplifier stages after the hollow-fiber system, however, complicates the system and reduces the spectral width of the continuum because of the limitation of the gain bandwidth. As a result, even though the continuum energy was as high as 3.5 mJ, the pulse duration was increased to 9.2 fs.

For the efficient suppression of the self-focusing and multi-photon ionization, a differentially pumped hollow-fiber system was proposed [8]. In the differentially pumped hollow fiber, the gas pressure varies from minimum at the entrance to maximum at the exit. Because the gas pressure is reduced to a few Torr at the entrance of the hollow fiber, the peak power of the input pulse can be increased without the self-focusing effect. While the laser pulse is propagating through the hollow fiber, the pulse energy decreases due to losses induced by multi-photon ionization and leakage, and the pulse duration increases due to the dispersion from both gas and waveguide, resulting in the reduction of the peak power. The self-focusing can thus be suppressed on the forward propagation of the laser pulse even though the critical power for the self-focusing decreases gradually by the increase of the gas pressure. As a result, the energy of the laser pulse propagated through the differentially pumped hollow-fiber compressor can be increased to multi-mJ because the self-focusing and serious energy loss due to multi-photon ionization can be suppressed.

In this paper we demonstrate the effectiveness of the differentially pumped hollow-fiber chirped-mirror compressor combined with the 1-kHz CPA Ti:sapphire laser system. The compressor produces two-cycle optical pulses with energy over 1 mJ as a result of efficient suppression of self-focusing and ionization.

## 2 1 kHz CPA laser system setup

The 1-kHz, high-power, femtosecond Ti:sapphire laser consisted of a long-cavity laser oscillator, a stretcher, two multi-pass amplifiers and a compressor. The seed pulses for the amplifiers were generated from a prism-dispersion-controlled femtosecond Ti:sapphire oscillator running at

✉ Fax: +82-62-970-3389, E-mail: sungjh@gist.ac.kr

27 MHz [9]. The oscillator was pumped by a frequency-doubled, diode-pumped Nd:YVO<sub>4</sub> laser (Spectra Physics). Laser pulses from the oscillator were stretched to about 220 ps by an aberration-free all-reflective Öffner-triplet-type stretcher, in which a grating with 1400 grooves/mm was used. Pulses then passed through an acousto-optic programmable dispersive filter (Dazzler, Fastlite), which controlled simultaneously the spectral amplitude and phase of the laser pulses, and through a Faraday isolator to block the backward ASE from the amplifiers.

The pulse was then injected into an 8-pass pre-amplifier. The amplifier consisted of three dielectric-coated flat mirrors and two dielectric-coated focusing mirrors with 90-cm radius of curvature. The two curved mirrors were placed in a confocal geometry. The pre-amplifier was pumped by 10-mJ green laser pulses from a diode-pumped *Q*-switched frequency-doubled Nd:YLF laser (Darwin, Quantronix). The seed beam was focused into the crystal by the first curved mirror, recollimated by the second curved mirror, and then directed toward the flat mirrors. After the first four passes, the preamplified pulse train was extracted from the amplifier, and pulses were selected using a Pockels cell at 1-kHz repetition rate. The selected pulses were then reinjected into the amplifier and their energy was boosted up to 1.4 mJ in the following four passes. The amplified pulses from the pre-amplifier were passed through another Pockels cell to minimize ASE and feedback and to enhance the contrast ratio.

The pulses from the preamplifier were further amplified in a 4-pass amplifier. This 4-pass amplifier was pumped by 30-mJ green laser pulses from a residual pump pulse of the 1st Nd:YLF laser and 20-mJ green laser pulses from a second *Q*-switched frequency-doubled Nd:YLF laser (Falcon, Quantronix). When a pump power of 30 W is used, one of major problems is thermal lensing induced by the heat load in the amplifier crystal. The thermal lensing can induce a mismatch between the pump beam and amplified beam modes in subsequent passes, resulting in strong thermal aberrations. Thus, in order to obtain good beam quality and sufficient amplification efficiency, we introduced the thermal eigenmode amplifier [10, 11], in which the size of the amplified beam can be kept up on the crystal. The output pulse energy reached 7.4 mJ while preserving a good spatial quality. The amplified pulses from the 4-pass amplifier were double-passed through two parallel gratings that had 1480 grooves/mm. For the elimination of thermal distortion and optical damage on the gratings, the beam diameter was expanded to 25 mm by using a convex/concave mirror pair. After compression, optical pulses with an energy of 4.5 mJ and a pulse duration of 26 fs were obtained.

### 3 Pulse compression to two-cycle pulses

For further pulse compression, the amplified 26-fs pulses were sent to a gas-filled hollow-fiber pulse compressor that employed a differentially pumped gas chamber [12]. A schematic diagram of the differentially pumped hollow-fiber compressor is shown in Fig. 1. The laser pulses from the kHz CPA laser were launched into a hollow fiber placed inside a gas chamber. The fiber was kept straight in a V-groove made on an aluminum bar placed in the chamber. The chamber had

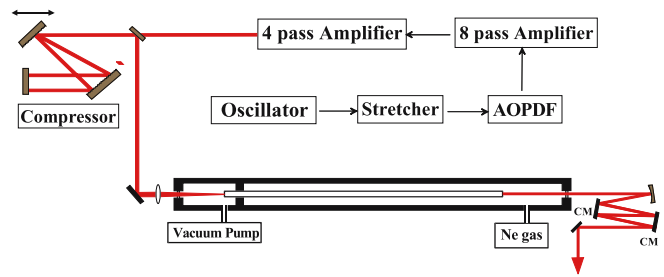


**FIGURE 1** Schematics of the kHz CPA Ti:Sapphire laser with a differentially pumped hollow-fiber pulse compressor. AOPDF, Acousto-optic programmable dispersive filter; CM, Chirped Mirror

1-mm-thick fused-silica windows with broadband antireflection coating at both surfaces. As shown in Fig. 1, the entrance side of the chamber is separated from the exit one in order to maintain a pressure gradient in the chamber. Through this separation, the exit side was filled with a gas while the entrance side was evacuated. As a result, the gas pressure was minimum at the entrance of the hollow fiber and maximum at the exit, resulting in a gas-pressure gradient inside the hollow fiber.

Any air fluctuations in the laser beam path can affect the spectral and spatial characteristics of laser pulses. This is also true for the propagation of laser pulses in the hollow-fiber compressor. We observed that the gas flow in the region between the entrance window and fiber input face affected the output spectral profile. The output spectral profile fluctuated when the gas outlet was located between the entrance window and the fiber input face. Thus, to avoid the gas fluctuations we placed the gas outlet close to the fiber input face.

When the high-power laser pulse is launched into the hollow fiber, the beam spot size, the gas type and its pressure should be chosen carefully for efficient suppression of self-focusing and multi-photon ionization. Self-focusing can be suppressed by increasing the critical power for self-focusing,  $P_{cr} = \lambda_0^2 / (2\kappa_2 p)$ , where  $\lambda_0$  is the central wavelength and  $\kappa_2$  is the ratio between the nonlinear index coefficient and the gas pressure  $p$  [6, 13]. Ionization can be avoided by increasing the beam spot size. The hollow-fiber diameter changes in proportion to the beam spot size for the optimum coupling efficiency. The larger the hollow-fiber diameter is, the longer the hollow fiber would become for maintaining low gas pressure at the entrance of the hollow fiber. Therefore, a gas with a high threshold for multi-photon ionization is preferable because it allows the use of small beam spot size and short hollow fiber. When argon gas was used as a nonlinear medium with about 0.2-TW input pulse, the hollow-core fiber should have a inner diameter of around 500  $\mu\text{m}$  for the ionization suppression. If 0.2-TW laser pulses are launched into the argon-filled hollow fiber with an inner diameter of less than 300  $\mu\text{m}$ , large ionization losses and strong plasma nonlinearity will be induced by the strong multi-photon ionization due to the high peak intensity of  $7 \times 10^{14} \text{ W/cm}^2$ . Recently, it was reported that 9.8-fs, 5-mJ optical pulses were generated using a 500- $\mu\text{m}$ -diameter 2.2-m-length hollow-core fiber when argon gas was used at 0.4 bar in the exit side of the chamber with 40-fs, 8.5-mJ input pulses [12]. In our experiments, neon gas which has a higher critical power was used at gas pressure in the range of 1–2 bar in the exit side of the chamber

in order to suppress the self-focusing and the ionization and achieve the spectral broadening for 2-cycle pulses with a comparatively short hollow fiber. At the exit the critical power for the self-focusing was as high as about 220 GW with 2.0-bar neon gas at a central wavelength of 810 nm. The neon pressure was lower than 1.0 torr in the entrance side when the hollow fiber had an inner diameter of 300  $\mu\text{m}$  and a length of 100 cm

For an optimal spectral broadening the frequency chirp of the laser pulse had to be controlled in order to compensate for the material dispersion in the focusing lens and the window. The laser chirp was controlled by adjusting the grating separation of the pulse compressor in the kHz CPA laser. The input pulse energy was 4.5 mJ and the neon pressure was 1.1 bar at the exit of the chamber. Figure 2 shows the laser spectra after the hollow-fiber pulse compressor with respect to the grating separation,  $\Delta L$ .  $\Delta L = 0$  corresponds to the grating separation that produces the shortest pulse after the grating compressor, and negative (positive) displacement of  $\Delta L$  corresponds to a positive (negative) frequency chirp. Because the positive frequency chirp is induced when laser pulses pass through the focusing lens and the 1-mm-thick window of the gas chamber, the laser pulses arriving at the fiber have positive frequency chirp at  $\Delta L = 0$ . As shown in Fig. 2, the laser spectrum at  $\Delta L = 60 \mu\text{m}$  has the broadest bandwidth. It means that the spectral broadening was optimized when the input pulse had a negative frequency chirp. With the groove density of the grating, incident and diffracted angles in the grating compressor, the calculated group delay dispersion (GDD) per 1- $\mu\text{m}$  displacement is  $-32 \text{ fs}^2$ . Because the total GDD value of the lens and window is about  $1800 \text{ fs}^2$ , the actual incident pulse will have the shortest pulse width at around  $\Delta L = 56 \mu\text{m}$ . This value agrees well with the condition of the broadest laser spectrum. Consequently, the spectral broadening was optimized by applying negatively chirped laser pulses in order to compensate for the positive chirp induced in the focusing lens and window.

When the spectral broadening was optimized, the output pulse energy was 1.4 mJ. In this condition of broad output

spectrum, sufficient to support 4.6-fs pulse, the coupling efficiency was 31%. The coupling efficiency could be increased to 40% at  $\Delta L = -40 \mu\text{m}$ , but the output spectrum was not as broad as the optimized one, only to support 6.2-fs pulse, as shown in Fig. 2. The low coupling efficiency resulted mainly from the multi-photon ionization loss. Because the hollow fiber used had 300- $\mu\text{m}$  diameter, the peak laser intensity was  $5 \times 10^{14} \text{ W/cm}^2$ . This high laser intensity induced the strong multi-photon ionization, resulting in the ionization loss. Thus, in order to increase the coupling efficiency the multi-photon ionization should be suppressed by increasing the beam spot size. This can be realized by increasing the hollow-fiber diameter to more than 400  $\mu\text{m}$  and the fiber length to longer than 1 m in order to avoid the increase of gas pressure at the fiber entrance and heavy gas loss due to the larger fiber diameter. The distance between the entrance window of the gas chamber and the fiber input face should become longer to prevent damage to the entrance window, resulting in a much longer gas chamber. In our experiment, the longer hollow fiber with larger inner diameter could not be installed because of the space limitation in the optical table.

Even broader laser spectrum could be obtained by applying higher laser intensity. When the spot size of input pulse was decreased by about 20%, compared to the optimal size, the laser spectrum became broader, but the amplitude modulation was much stronger as shown in Fig. 3, and the output energy was reduced to less than 1 mJ with 0.77-bar neon in the exit. The strong modulation and low output energy originate from the high laser intensity. The high-intensity laser pulses generate the strong multi-photon ionization and thus the ionization losses become large, and the spectrum is broadened by the ionization-induced plasma nonlinearity as well as Kerr nonlinearity [14]. This strong spectral modulation will induce more pronounced wings on the temporal profile of the laser pulse after dispersion compensation. Thus, in order to obtain a relatively clean temporal profile after dispersion compensation, an optimal laser intensity should be chosen.

We also compared the laser characteristics with those of the static gas fill case. When the hollow fiber was filled with

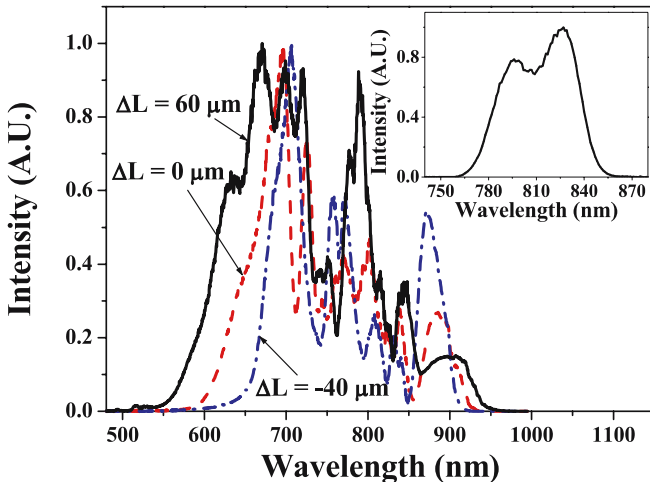


**FIGURE 2** Laser spectra after passing through the hollow-fiber compressor with respect to the grating separation  $\Delta L$  of the pulse compressor in the kHz CPA Ti:Sapphire laser.  $\Delta L = 0$  corresponds to the grating separation of the shortest pulse after the grating compressor. The *inset* shows the laser spectrum before the hollow fiber

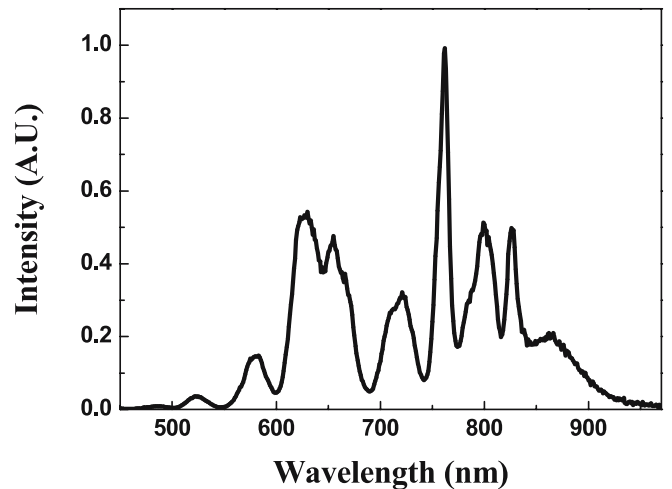


**FIGURE 3** Laser spectrum after passing through the differentially pumped hollow fiber with an applied laser intensity of  $7 \times 10^{14} \text{ W/cm}^2$  and the neon pressure of 0.8 bar

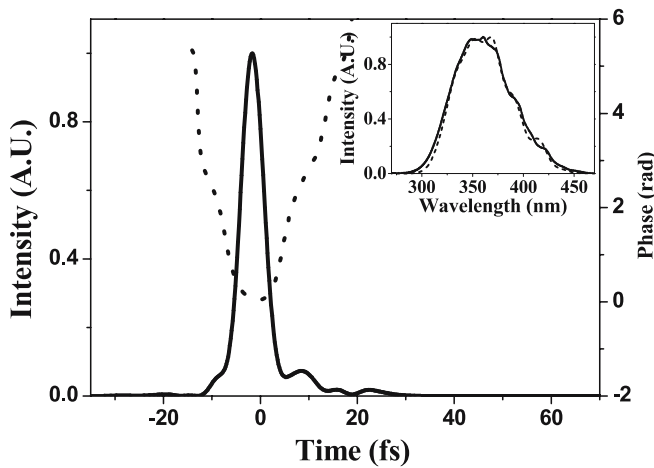


**FIGURE 4** Intensity and phase profiles of the compressed pulse, retrieved from SHG FROG. The *inset* shows the SHG FROG frequency marginal (*dashed curve*) and the autoconvolution (*solid curve*) of the measured fundamental spectrum

0.9-bar neon gas without differential pumping, the spectrum was similar to that shown in Fig. 2. But, the energy of the output pulse in this case was less than 0.9 mJ. This low output energy is the result of losses due to multi-photon ionization. Compared with the differential pumping method, the ionization losses are larger because of the high gas density at the entrance of the hollow fiber. As a result, amplifier stages after the hollow-fiber system will be needed to increase the pulse energy to more than 1 mJ in the static gas fill case. The static hollow-fiber system, however, has more complexity than the differentially pumped hollow-fiber system due to the addition of amplifier stages and the reduced spectral width of the continuum, as stated in Sect. 1. Recently, the generation of few-cycle laser pulses with a good spatial profile through filamentation was demonstrated [15]. However, in order to apply this technique to a laser with multi-mJ energy the problem associated with multiple filamentations has to be overcome.

After recollimation by a silver mirror of 1-m focal length, the laser pulses were reflected four times by a pair of chirped mirrors for dispersion compensation. The chirped mirrors had a high reflectivity over the wavelength range of 600–1000 nm and a constant negative GDD of  $-45 \text{ fs}^2$  between 600 and 950 nm. The final energy of the laser pulses after the chirped mirrors was around 1.1 mJ. The pulse duration was evaluated using the second-harmonic generation (SHG) frequency resolved optical gating (FROG) method [16]. In the SHG FROG, a 10- $\mu\text{m}$ -thick  $\beta$ -barium borate crystal was used in the type I geometry for sufficient phase-matching bandwidth.

The measured pulse duration was 5.5 fs, and the good agreement between the autoconvolution of the fundamental spectrum and the SHG FROG marginal was obtained as shown in Fig. 4.

#### 4 Conclusion

We generated high-energy 2-cycle laser pulses using a differentially pumped hollow-fiber chirped-mirror compressor in which the self-focusing and losses due to ionization could be suppressed effectively. The laser spectrum after the hollow-fiber compressor was optimized by controlling the laser chirp, in order to compensate for the material dispersion in a focusing lens and a window, and extended from 540 nm to 950 nm. The spectrally broadened laser pulses were compressed to 5.5 fs by a pair of chirped mirrors and had a final energy of 1.1 mJ. These 1-kHz 0.2-TW 2-cycle pulses are well suited for attosecond physics investigations through high harmonic generation and for research on various nonlinear processes in which intense few-cycle laser pulses play an important role.

**ACKNOWLEDGEMENTS** The authors greatly appreciate K. Midorikawa and A. Suda for helpful discussion. This work is supported by the Ministry of Science and Technology of Korea through the Creative Research Initiative Program.

#### REFERENCES

- 1 Y. Nabekawa, Y. Kuramoto, T. Togashi, T. Sekikawa, S. Watanabe, *Opt. Lett.* **23**, 1384 (1998)
- 2 M. Nisoli, S. De Silvestri, O. Svelto, *Appl. Phys. Lett.* **68**, 2793 (1996)
- 3 M. Nisoli, S. De Silvestri, O. Svelto, R. Szepocz, K. Ferencz, C. Spielmann, S. Sartania, F. Krausz, *Opt. Lett.* **22**, 522 (1997)
- 4 S. Sartania, Z. Cheng, M. Lenzner, G. Tempea, C. Spielmann, F. Krausz, *Opt. Lett.* **22**, 1562 (1997)
- 5 G. Tempea, T. Brabec, *Opt. Lett.* **23**, 762 (1998)
- 6 N. Milosevic, G. Tempea, T. Brabec, *Opt. Lett.* **25**, 672 (2000)
- 7 J. Seres, A. Müller, E. Seres, K. O'Keeffe, M. Lenner, R.F. Herzog, D. Kaplan, C. Spielmann, F. Krausz, *Opt. Lett.* **28**, 1832 (2003)
- 8 M. Nurhuda, A. Suda, K. Midorikawa, M. Hatayama, K. Nagasaka, *J. Opt. Soc. Am. B* **20**, 2002 (2003)
- 9 J.H. Sung, K.H. Hong, Y.H. Cha, C.H. Nam, *Jpn. J. Appl. Phys.* **41**, 931 (2002)
- 10 R. Salin, C.L. Blanc, J. Squier, C. Barty, *Opt. Lett.* **23**, 718 (1998)
- 11 C.L. Blanc, E. Baubeau, F. Salin, J.A. Squier, C.P.J. Barty, C. Spielmann, *IEEE J. Quantum Electron.* **4**, 407 (1998)
- 12 A. Suda, M. Hatayama, K. Nagasaka, K. Midorikawa, *Appl. Phys. Lett.* **86**, 111 116 (2005)
- 13 C. Vozzi, M. Nisoli, G. Sansone, S. Stagira, S. De Silvestri, *Appl. Phys. B* **80**, 285 (2004)
- 14 G. Tempea, T. Brabec, *Opt. Lett.* **23**, 1286 (1998)
- 15 C.P. Hauri, W. Kornelis, F.W. Helbing, A. Heinrich, A. Couairon, A. Mysyrowicz, J. Biegeri, U. Keller, *Appl. Phys. B* **79**, 673 (2004)
- 16 Z. Cheng, A. Furbach, S. Sartania, M. Lenzner, C. Spielmann, F. Krausz, *Opt. Lett.* **24**, 247 (1999)